Mitigation of Subsynchronous Resonance in a Series-Compensated Wind Farm Using FACTS Controllers

Rajiv K. Varma, *Member, IEEE*, Soubhik Auddy, *Student Member, IEEE*, and Ysni Semsedini

***Abstract*—The rapid growth of wind power systems worldwide will likely see the integration of large wind farms with electrical networks that are series compensated for ensuring stable transmission of bulk power. This may potentially lead to subsynchronous-resonance (SSR) issues. Although SSR is a well-understood phenomenon that can be mitigated with flexible ac transmission system (FACTS) devices, scant information is available on the SSR problem in a series-compensated wind farm. This paper reports the potential occurrence and mitigation of SSR caused by an induction-generator (IG) effect as well as torsional interactions, in a series-compensated wind farm. SSR suppression is achieved as an additional advantage of FACTS controllers which may already be installed in the power system for achieving other objectives. In this study, a wind farm employing a self-excited induction generator is connected to the grid through a series-compensated line. A static var compensator (SVC) with a simple voltage regulator is first employed at the IG terminal in addition to the fixed shunt capacitor for dynamic reactive power support. The same SVC is shown to effectively damp SSR when equipped with an SSR damping controller. Also, a thyristor-controlled series capacitor (TCSC) that is actually installed to increase the power transfer capability of the transmission line is also shown to damp subsynchronous oscillations when provided with closed-loop current control. While both FACTS controllers—the SVC and TCSC—can effectively mitigate SSR, the performance of TCSC is shown to be superior. Extensive simulations have been carried out using EMTDC/PSCAD to validate the performance of SVC and TCSC in damping SSR.**

***Index Terms*—Flexible ac transmission systems (FACTS), self-excited induction generator (SEIG), series compensation, static VAR compensator (SVC), subsynchronous resonance (SSR), thyristor-controlled series capacitor (TCSC), wind power systems.**

I. Introduction

ENVIRONMENTAL pollution and shortage of conventional fossil fuel are the two major concerns which have led to the global emergence of wind energy as an effective means of power production. Wind generating capacities have increased from negligible levels in the early 1990s to more than 50 GW today [1], [2]. This shift to wind energy will inevitably lead to large wind turbine generators (WTGs) being integrated into electric power grids. It will be further necessary to transmit the generated power through transmission networks that can sustain large power flows. It is well known that series compensation is an effective means of increasing power transfer capability of an existing transmission network. However, series compensation is shown to cause a highly detrimental phenomenon called subsynchronous resonance in electrical networks [3], [4].

Flexible ac transmission systems (FACTS) can provide an effective solution to alleviate SSR [5]–[9] and thyristor-based FACTS controllers have been employed in the field for this purpose [10], [11]. Wind turbines are subject to mechanical modes of vibrations related to turbine blades, shaft, gear train, tower, etc. [12], [13]. In the case of wind turbine generators operating radially on the end of a series-compensated transmission line, there is the potential for induction-machine self-excitation SSR [14], [15].

The main motivation behind this work is to utilize thyristor-based FACTS devices for mitigation of SSR. The FACTS devices may be already installed for achieving other objectives and SSR damping function can be additionally included, or the FACTS devices can be exclusively connected for mitigating SSR. For instance, an SVC may be already located at the wind farm for dynamic reactive power support or for other power-quality (PQ) improvement purposes. Similarly, a TCSC may already be inserted in the transmission network to increase the power transfer capability, and the large capacity wind farm may now need to evacuate power through this series-compensated network.

In this paper, both an SVC at the wind farm terminal and a TCSC in series with the line are applied to damp subsynchronous oscillations. The SVC performance is examined with both voltage controller and an auxiliary SSR damping controller (SSRDC). The TCSC is equipped with a current controller. The performance of SVC and TCSC in damping SSR is investigated over a wide range of operating conditions.

The organization of the paper is as follows. The two mechanisms of SSR—induction generator (IG) and torsional interaction (TI) effects—are briefly described in Section II. Section III outlines the study system configuration. Section IV proves the potential occurrence of SSR both due to IG and TI effects in a series-compensated wind farm. Section V covers the control system design of the SVC and TCSC. The performance of the SVC in mitigating SSR is shown in Section VI. The comparative performance of SVC and TCSC in obviating SSR is presented in Section VII. Finally, Section VIII concludes this paper.

Manuscript received September 19, 2006; revised April 11, 2007. Paper no. TPWRD-00567-2006.

R. K. Varma and S. Auddy are with the Electrical and Computer Engineering Department, University of Western Ontario (U.W.O), London, ON N6A 5B9 Canada (e-mail: rkvarma@uwo.ca; sauddy@uwo.ca).

Y. Semsedini is with London Hydro, London, ON N6A 4J8, Canada (e-mail: semsediy@LondonHydro.com).

Color versions of one or more of the figures in this paper are available online at http://ieeexplore.ieee.org.

Digital Object Identifier 10.1109/TPWRD.2008.917699

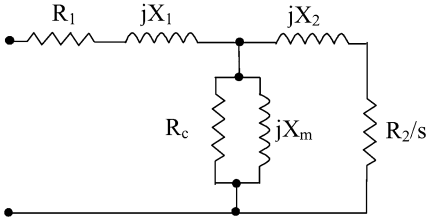

Fig. 1. Equivalent circuit diagram of a generic induction machine. $\mathrm{R}_1 =$ the stator resistance, $\mathrm{X}_1 =$ the stator leakage reactance, $\mathrm{R}_2 =$ the rotor resistance referred to stator, $\mathrm{X}_2 =$ the rotor leakage reactance referred to stator, $\mathrm{R}_\mathrm{c} =$ the core-loss resistance, and $\mathrm{X}_\mathrm{m} =$ the magnetizing reactance.

II. Subsynchronous Resonance

Subsynchronous resonance occurs in a power system network when the mechanical system of the generator exchanges energy with the electrical network [3], [4]. Series compensation in the line results in excitation of subsynchronous currents at an electrical frequency f_e given by

$$f_e = f_0\sqrt{\frac{x_c}{x_\Sigma}} \tag{1}$$

where x_c is the reactance of the series capacitor, x_Σ is the reactance of the line including that of the generator and transformer, and f_0 is the nominal frequency of the power system.

These currents result in rotor torques and currents at the complementary frequency f_r as

$$f_r = f_0 - f_e. \tag{2}$$

These rotor currents result in subsynchronous armature voltage components which may enhance subsynchronous armature currents to produce SSR. There are two aspects of the SSR.

1) Self excitation involving both an induction generator effect and torsional interaction.
2) Transient torque (also called transient SSR).

A. Induction Generator Effect

Self-excitation of the electrical system alone is caused by the induction generator effect. This can be explained in the case of a wind farm comprising self-excited induction generators (SEIGs) from the generic equivalent circuit of an SEIG drawn in Fig. 1. As the rotating mmf produced by the subsynchronous frequency armature currents moves at speed N_s, which is slower than the speed of the rotor N_r, the resistance of the rotor (at the subsynchronous frequency viewed from the armature terminals) is negative, as the slip " s " of the induction generator is negative. This is clear from the equivalent circuit shown in Fig. 1

$$s = \frac{N_s - N_r}{N_s}. \tag{3}$$

When the magnitude of this resistance exceeds the sum of the armature and network resistances at a resonant frequency, there will be self-excitation, and the subsynchronous electrical current will tend to increase rapidly.

B. Torsional Interactions

This form of self excitation involves both electrical and mechanical dynamics. This may occur when the electrical resonant frequency f_e is near the complement of a torsional resonant frequency f_n of the turbine-generator (TG) shaft system [3], [4]. The torques at rotor torsional frequencies may then get amplified and potentially lead to shaft failure.

C. Transient SSR

Transient SSR generally refers to transient torques on segments of the $T-G$ shaft resulting from subsynchronous oscillating currents in the network caused by faults or switching operations. This usually occurs when the complement of the electrical network resonant frequency gets closely aligned with one of the torsional natural frequencies.

III. System Configuration

A. Choice of the System Parameters

Wind farms with tens or even hundreds of similar wind turbine generators (WTGs) have been erected, leading to large-scale wind power projects [1]. The choice of the study systems in this paper is based on the rating of wind farms functioning in Ontario, Canada, as well as the wind farms operational worldwide. In Ontario, 100-MW capacity wind farms are already in service, for instance, the Kings Bridge North II Wind Farm near Goderich and the Erie Shore Wind Farm at Port Burwell.

In the U.S., the King Mountain Wind Range in Upton County, TX, consists of 214 wind turbines of 1.3 MW each leading to a capacity of 278.2 MW [21]. Moreover, several alternatives of integrating 500 MW to 1000 MW conventional induction wind generations are being investigated into the Dakotas transmission system, for export to the Twin Cities, Wisconsin, Iowa, and Illinois [14]. In [20], a conventional synchronous generator is replaced with an equivalent 500-MVA rating wind turbine. Based on these practical systems, the system studies in this paper are conducted for a wind farm having a power output varying from 100 to 500 MW. Most studies are reported for a realistic wind power generation of 100 MW. Since a majority of existing WTGs are based on SEIGs [1], the studies in this paper are conducted with SEIG-based WTGs.

B. Actual Study System

The transmission network of the study system is derived essentially from the IEEE first benchmark model of SSR studies [16]. There are two separate systems which have been investigated. First of all, a set of coherent induction generators is connected to grid through a fixed series-compensated line which is depicted in Fig. 2. An appropriately large number of 1000-hp self-excited double-cage IGs [18] are assumed to be connected together in the wind farm to provide a net power output which can vary from 100 to 500 MW. As IGs do not have an internal excitation system, additional reactive support is needed to operate the IGs with a power factor in the range of 0.98–0.99 lagging [14]. Two study systems are considered. In Study System

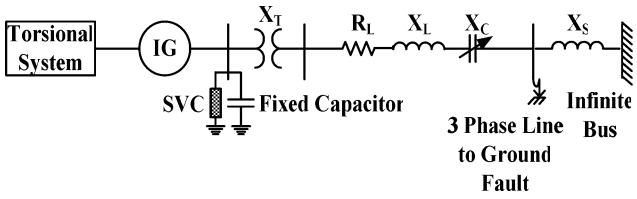

Fig. 2. Study System 1: WTG shunt compensated with SVC.

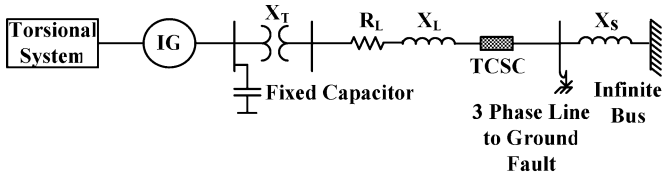

Fig. 3. Study System 2: WTG with the transmission line compensated by a TCSC.

1, an SVC is connected at the IG terminal for dynamic reactive power support.

In Study System 2, SVC is not considered. Instead, the series capacitor X_C is replaced with a TCSC as shown in Fig. 3. The capacitive reactance of the TCSC is the same as variable line series compensation. The detailed data for both study systems are presented in Appendix A.

IV. SSR in a Series-Compensated Wind Farm

In this section, both the IG self excitation and torsional interaction effects are studied in the Study System 1 depicted in Fig. 2. The system is first modified to remove the SVC so that the possibility of SSR can be examined in a non-FACTS-equipped series-compensated wind farm. A three-phase-to-ground fault is implemented to study the potential of self excitation and transient torque SSR. The power-flow studies are conducted using the DSA Power Tools software [17] and the electromagnetic time-domain simulations are performed with PSCAD/EMTDC software [18].

A. IG Self-Excitation Effect

The torsional system of the WTG is disabled in this investigation. Studies reported in this section show that there are two factors which influence the self-excitation phenomenon of an induction generator. These are:

- power output of the WTG;
- level of series compensation.

These factors are addressed separately.

1) Variation in Wind Generator Power Output: The electromagnetic torque is obtained for WTG power outputs of 100, 200, 300, and 500 MW to examine the onset of IG self-excitation. The results are depicted in Fig. 4. It is observed that for a power transfer "P" of 100 MW, the IG self-excitation effect is not so prominent even with a series compensation level $\mathrm{p} = 90\%$. Oscillations are visible in the electromagnetic torque but they decay with time. However, as the power transfer level is increased to 300 MW, oscillations of high magnitude appear in the electromagnetic torque. When the power transfer level reaches 500 MW, the oscillations start growing and eventually make the system unstable. At this high power level, the IG operates at a much higher speed over the synchronous speed. This increased power transfer makes the apparent negative rotor resistance exceed the sum of total armature and network resistance, thus giving rise to subsynchronous oscillations. The dominant electrical mode " f_e " in this case is 20.54 Hz.

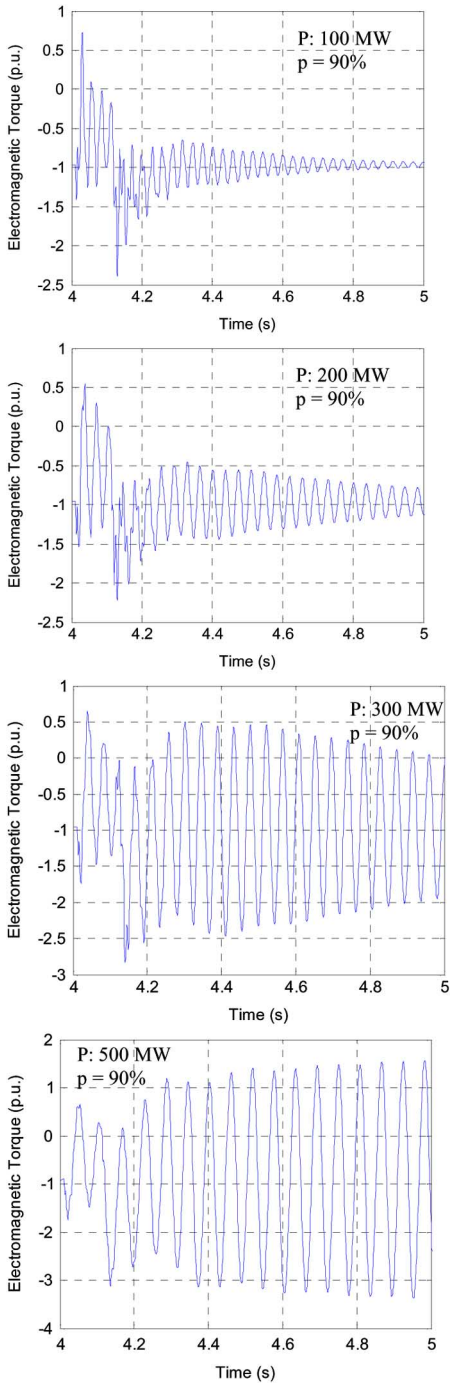

Fig. 4. Electromagnetic torque for different WTG power outputs and same series compensation level.

For each power-flow level, if the line resistance decreases, these oscillations become larger and continue for a longer duration which is expected of IG self-excitation oscillations. However, the line resistance reduction is not a realistic option and is hence not reported here.

2) Variation in Levels of Series Compensation: Next, the series compensation level is varied for 500-MW generator power

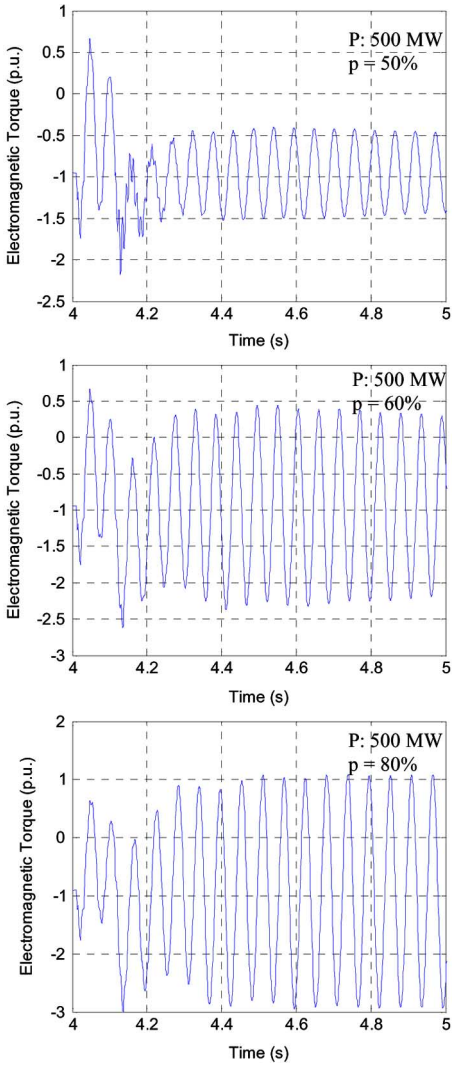

Fig. 5. Electromagnetic torque for different series compensation and the same power-flow level.

output. The electromagnetic torque is depicted for 50%, 60%, and 80% line compensation in Fig. 5 while that for 90% compensation is already illustrated in Fig. 4. It is observed that with increasing series compensation levels, the oscillations due to IG self excitation get enhanced, making the system eventually unstable. The electrical frequency f_e in the electromagnetic torque increases according to (1) and, consequently, the rotor torque frequency f_r decreases as in (2).

B. Torsional Interactions

A very high level of series compensation is typically needed as indicated by (1) and (2) to generate a rotor torque at a frequency in the close vicinity of the resonant frequency of the wind turbine mechanical system (comprising rotor blades and gear train). There are, in fact, two typical resonant frequencies [12], [13].

1) 1.1 Hz corresponding to the tower sideways oscillations.
2) 2.5 Hz relating to mechanical systems.

A two-mass torsional system model is added to the IG model in PSCAD [18]. Since both the frequencies are very close, only one torsional frequency is considered to represent the effect of both of these natural frequencies. Hence, Mass 1 models the combined tower and wind turbine mechanical system and Mass 2 represents the inertia of the generator.

In this case, varying levels of power flow as well as series compensation are considered to verify the existence of the torsional interactions.

1) Variation in Wind Generator Power Output: The WTG power output is varied with a very high level of series compensation of 90%. Fig. 6 depicts both the electromagnetic torque T_e and mechanical torque between mass 1 and mass 2, T_{12}, for varying levels of power flow of 50, 70, and 100 MW. It is observed that even at 70 MW power flow, the system becomes unstable with growing oscillations visible both in T_e and T_{12}.

2) Variation in Levels of Series Compensation: The mechanical torque T_{12} between Mass 1 and Mass 2 and electromagnetic torque T_e of the WTG are depicted for varying levels of series compensations of 50%, 65%, at 100 MW power flow in Fig. 7. The results for 90% are already displayed in Fig. 6. It is observed that with increasing series compensation levels, the oscillations due to torsional interaction also get enhanced by making the system eventually unstable even at realistic levels of compensation of 65% [3]–[5], [19]. In each case, the electromagnetic torque signal displays both the torsional mode and subsynchronous electrical mode oscillations superimposed on it.

V. Controller Design of SVC and TCSC

A. Controller Design of SVC

In Study System 1, the SVC is mainly used to regulate the wind farm bus voltage during disturbances in the system. An auxiliary subsynchronous resonance damping controller (SSRDC) is designed and added suitably to enhance the torsional-mode damping of the system. The general configuration of an SVC with its voltage regulator and auxiliary controller is shown in Fig. 8.

In this study, the voltage regulator is a simple PI controller whose proportional gain is set to zero. The integral gain is selected by a systematic hit-and-trial method using time-domain simulation [18] to give the best K_I, which results in a fast rise time and minimal settling time with acceptable overshoot (10%) in generator terminal voltage in response to a step change in the reference voltage $V_{\rm ref}$. The auxiliary controller $H(s)$ can take different structures depending on which control design technique is being employed [19]. The structure of the auxiliary subsynchronous damping controller (SSRDC) is shown in Fig. 9 where Δ *Sig* represents the incremental value of the auxiliary signal or the feedback signal. The different signals generally considered as input to the auxiliary controller are line real power flow, line current magnitude, bus frequency, bus voltage magnitude, etc. [6]. In this paper, the wind turbine generator speed deviation $(\Delta\omega)$ has been used as an auxiliary signal to damp the unstable modes.

The SSRDC comprises a simple proportional controller through a washout circuit. The purpose of washout circuit is to prevent the auxiliary controller from responding to steady-state power flow. The proportional gain of SSRDC is determined from a systematic hit and trial using the nonlinear time-domain

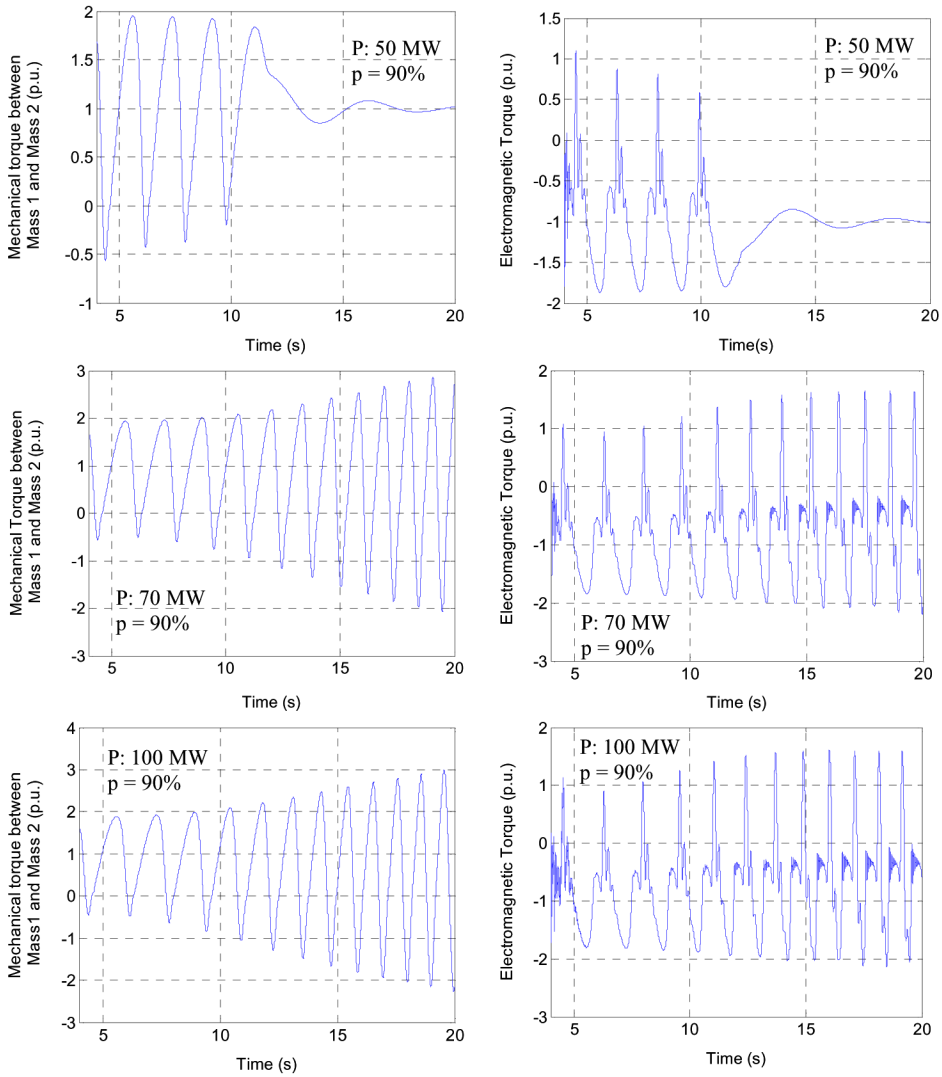

Fig. 6. Mechanical torque between mass 1 and mass 2 (T_{12}) and electromagnetic torque T_e for different power transfer levels at same series compensation.

simulation using PSCAD software to result in fastest settling time. The output of the SSRDC is then fed to the SVC voltage regulator as shown in Fig. 9.

B. Controller Design of TCSC

The TCSC increases the power transfer capability of a transmission network in addition to several other functions [5], [6]. It provides a rapid, continuous control of the transmission-line series compensation level thus dynamically controlling the power flow in the line.

In Study System 2, the TCSC is assumed to be primarily employed in the network for controlling line reactance and thereby the power flow. The SSR damping function is added through constant current control for this study. It is reported [9] that a TCSC operating at fundamental frequency offers a pure capacitive reactance to increase the power transfer capability of the network. On the other hand, the same TCSC offers resistive and inductive impedance at subsynchronous frequencies which assists in damping subsynchronous modes. The resistive impedance of the TCSC increases with the increased boost factor which is the ratio of the capacitive reactance offered by the TCSC and the total line reactance.

The general configuration of a TCSC will be shown next (Fig. 10). For this configuration, the equivalent TCSC reactance is computed per the following equation:

$$X_{\mathrm{TCSC}} = X_C - \frac{X_C^2}{X_C - X_L}\frac{2\beta + \sin 2\beta}{\pi} + \frac{4X_C^2}{X_C - X_L}\frac{\cos^2\beta}{k^2 - 1}\frac{k\tan k\beta - \tan\beta}{\pi} \quad (4)$$

where $\beta =$ the angle of advance (before the forward voltage becomes zero) $= \pi - \alpha; \alpha$ is the firing angle of the thyristors. It is noted from (4) that a parallel resonance is created between X_C and X_L at the fundamental frequency, corresponding to the values of firing angle α_{res}, given by

$$\alpha_{\mathrm{res}} = \pi - (2m-1)\frac{\pi\omega}{2\omega_r}. \quad (5)$$

The different resonances can be reduced to only one by proper choice of $k = \omega_r/\omega = \sqrt{(\mathrm{X_C/X_L})}$ in the range 90 ° <

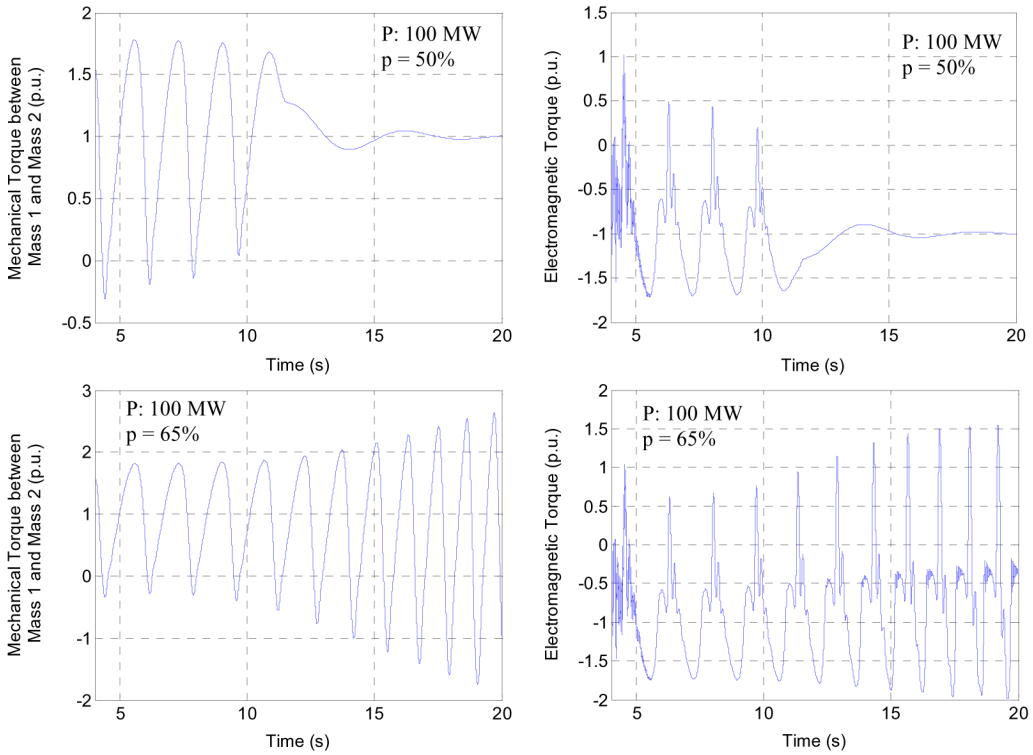

Fig. 7. Mechanical torque between mass 1 and 2 (T_{12}) and electromagnetic torque T_e for different series compensation and same power flow; $f_r = 0.8$ Hz.

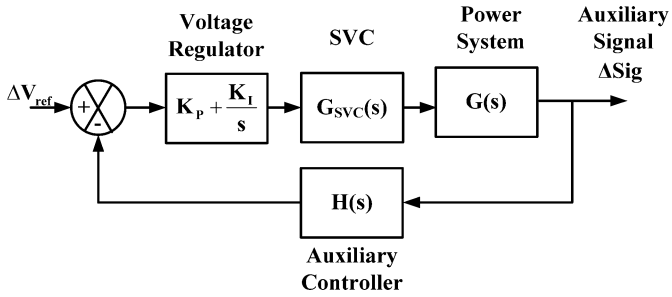

Fig. 8. Generalized SVC auxiliary control.

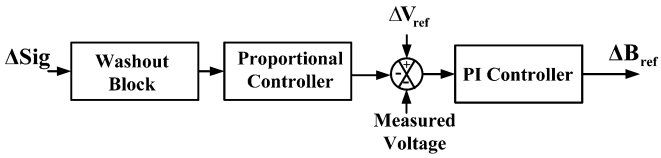

Fig. 9. Structure of SVC subsynchronous resonance damping controller (SSRDC).

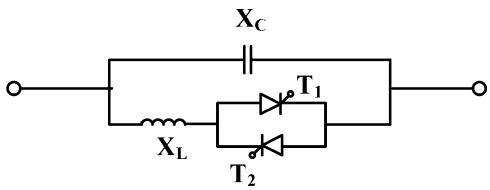

Fig. 10. General configuration of a TCSC.

$\alpha < 180^0$. As X_C is known, X_L can be calculated once a proper value of k is chosen to ensure a single resonant peak. Once the X_C and X_L values of the TCSC are computed, a closed-loop current control scheme is employed for the proposed application. The functional block diagram of TCSC is depicted in Fig. 11.

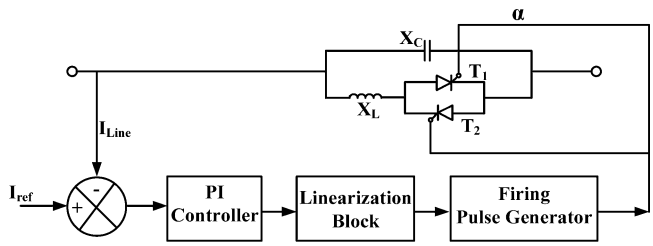

Fig. 11. TCSC constant current controller.

Here, $I_{\rm ref}$ is the prefault or precontingency current calculated from EMTDC/PSCAD line-current phasor. The main current controller is a PI controller. The parameters of this controller are also adjusted systematically through electromagnetic transient simulation studies by systematic hit-trial to obtain the minimum settling time or fastest damping.

VI. Performance of SVC in the Mitigation of SSR

Having demonstrated before that the SSR phenomenon can potentially exist in the series-compensated wind farms, the damping of subsynchronous oscillations (SSO) through SVC control is now considered in this section.

A. Damping of IG Effect

The performance of the SVC in alleviating the IG effect is evaluated at the worst possible operating point of 500-MW power transfer and 90% series compensation level. Fig. 12 depicts signals below with and without the SVC voltage regulator:

- electromagnetic torque of the generator (T_e);
- generator rotor speed (ω_r);
- generator terminal voltage (V_t);
- SVC reactive power ($Q_{\rm SVC}$).

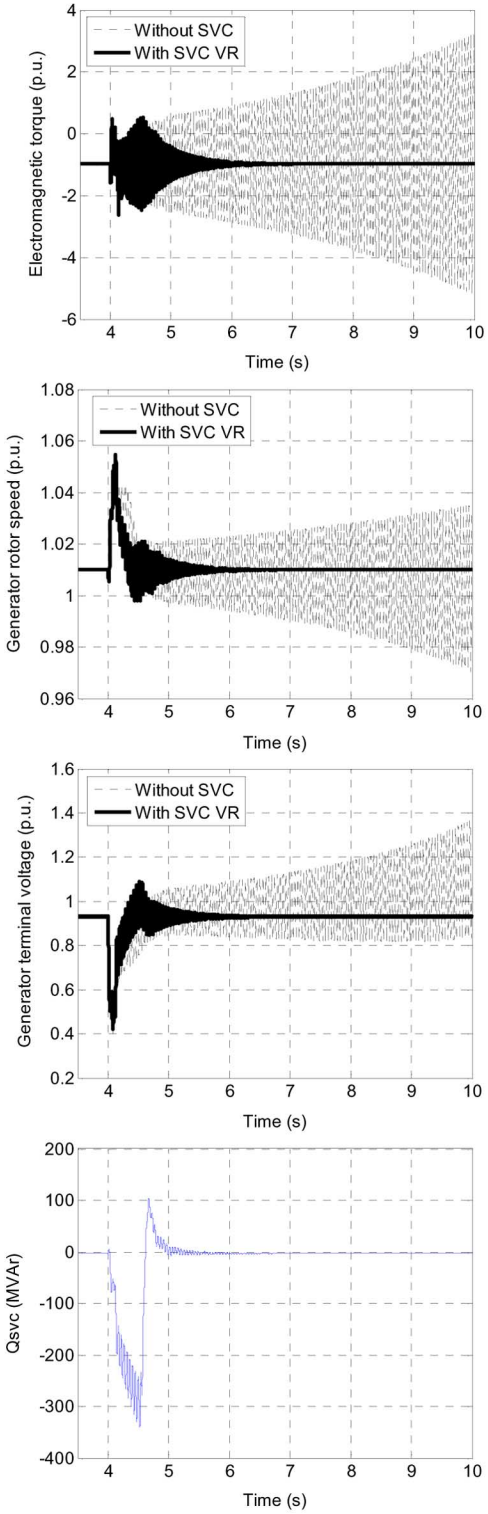

Fig. 12. Performance of SVC in damping SSO due to the IG effect.

B. Damping of TI Effect

Torsional interactions become prominent at a power transfer level of 100 MW. As a result, the damping performance of SVC with respect to the TI effect is shown at 100-MW power flow and 90% series compensation. The signals reporting to demonstrate the damping performance of SVC are:

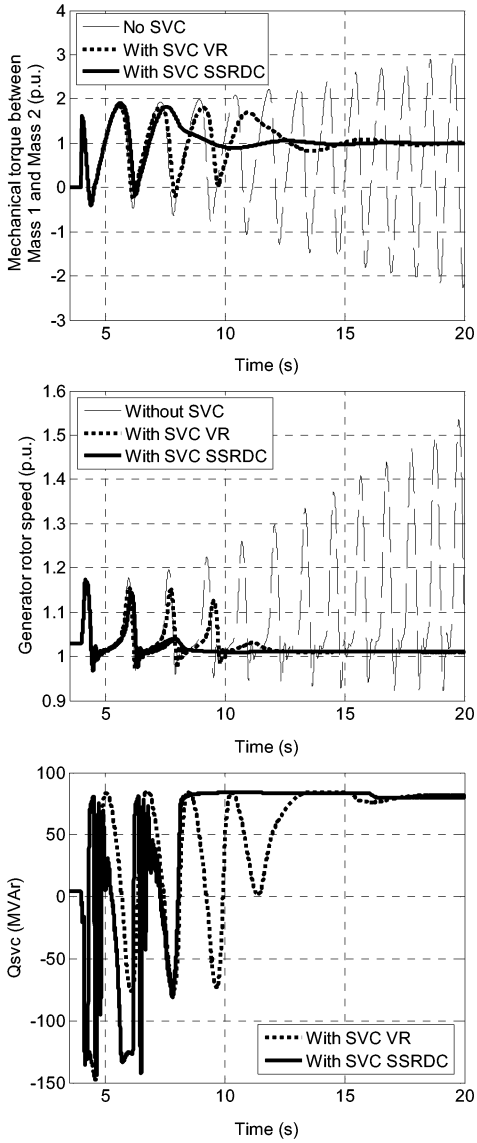

Fig. 13. Performance of SVC in damping SSO due to the TI effect.

- mechanical torque between Mass 1 and Mass 2 (T_{12});
- generator rotor speed (ω_r);
- SVC reactive power $(Q_{\rm SVC})$.

The impact of the SVC voltage regulator and SSRDC is displayed in Fig. 13. It is observed that the SVC voltage regulator damps the SSO due to the TI effect. Moreover, the damping is substantially enhanced by SSRDC of the SVC.

VII. Performance of TCSC in the Mitigation of SSR and Comparison With SVC

Intuitively, a series device can directly influence the line impedance of a network unlike a shunt device which always imparts a reactance in parallel with the network. As mentioned in Section V, increasing the TCSC series compensation offers a more resistive and inductive impedance at subsynchronous frequencies. Since TCSC is a series device, more resistance will directly add on to the line impedance improving the system damping. From these two factors, TCSC is expected to be more effective in damping SSR both due to torsional interactions and

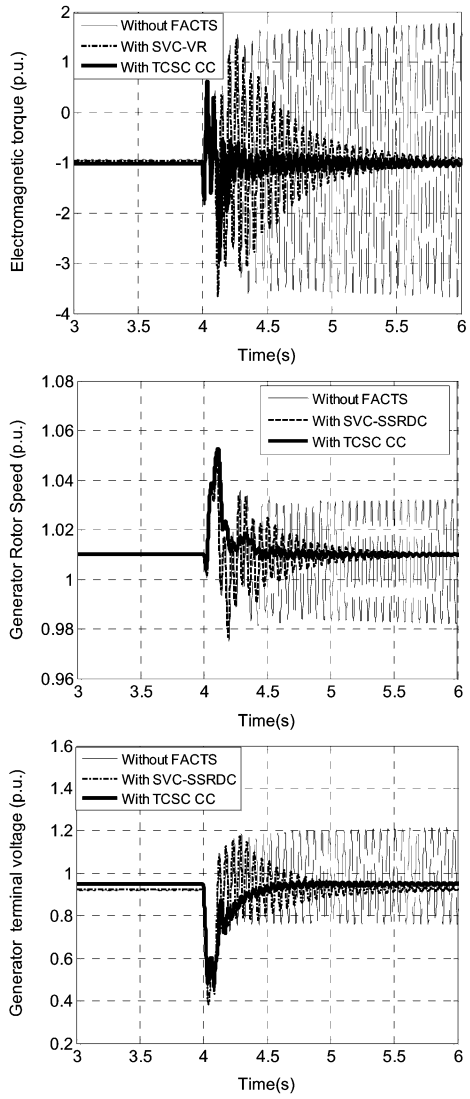

Fig. 14. Performance comparison of the SVC and TCSC in damping SSO due to the IG effect.

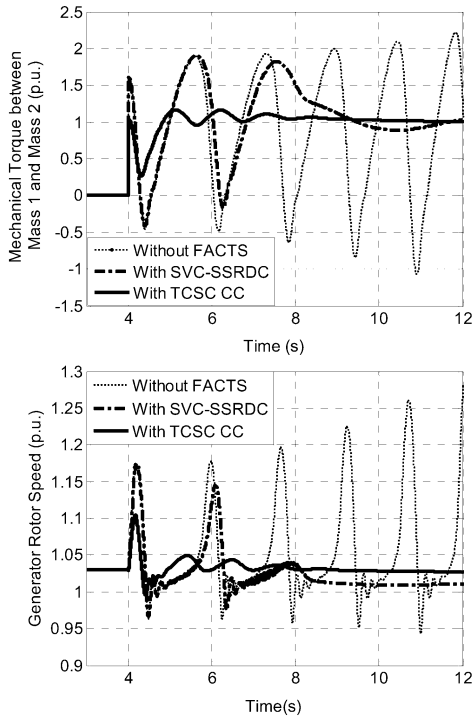

Fig. 15. Performance comparison of SVC and TCSC in damping TI.

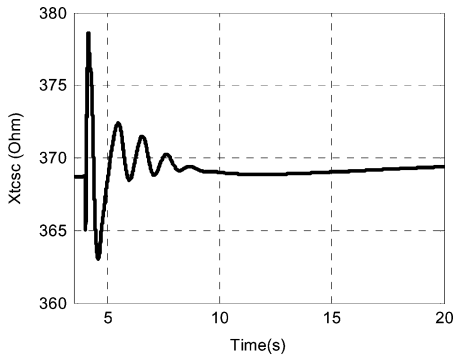

Fig. 16. Variation of TCSC reactance in damping of the SSO.

IG effects. The following figures compare the performance of the TCSC and SVC in damping the IG and TI effects. In case of torsional interactions, TCSC closed-loop current control performs even better than the SSRDC of the SVC.

A. Damping of the IG Effect

In this case, the damping performance of the TCSC is shown for the worst possible operating condition of 500-MW power flow and 90% series compensation. The signals utilized for examining the damping performance of TCSC are:

- electromagnetic torque of the generator (T_e);
- generator rotor speed (ω_r);
- generator terminal voltage (V_t).

These signals are depicted in Fig. 14 for the cases—without any FACTS device, with an SVC voltage regulator (VR), and with the TCSC current controller (CC).

The performance of TCSC is clearly superior in damping SSO due to the IG effect for the case of 90% series compensation.

B. Damping for TI Effect

Finally, the damping of TCSC in mitigating torsional interaction is investigated. The signals examined are:

- mechanical torque between Mass 1 and Mass 2 (T_{12});
- generator rotor speed (ω_r);
- TCSC reactance (X_{TCSC}).

The first two signals are plotted in Fig. 15 for the cases—without any FACTS device, with SVC–SSRDC, and with TCSC–CC. Even though the SVC auxiliary controller for SSR (SSRDC) improves the damping of the mechanical torque between Mass 1 and Mass 2, the TCSC closed-loop control provides much faster damping. The variation of TCSC reactance in damping SSO is depicted in Fig. 16.

VIII. Conclusion

With the rapid growth of wind power penetration into the power system grid, wind farms will likely be evacuating bulk

power through series-compensated networks. This will render the power system vulnerable to SSR. In this paper, two thyristor-based FACTS devices—SVC and TCSC—are applied to damp SSR in this type of series-compensated wind farm. The following conclusions are drawn from extensive electromagnetic transient simulation studies over widely varying levels of power flow and series compensation.

- SSR is a potential threat in series-compensated wind farms even at realistic levels of series compensation and practical levels of power flow.
- SVC and TCSC are both effective in damping subsynchronous oscillations due to torsional interaction as well as induction generator effects, when the system is subjected to a severe fault.
- SVC–SSRDC provides improved damping of the torsional interactions compared to a pure SVC voltage regulator.
- TCSC current control is better than SVC in mitigating SSR even when the SVC is equipped with the SSRDC.

In this paper, the possibility of SSR occurrence is studied with self-excited induction generators (SEIG)-based wind farms. Studies are presently being conducted to investigate the SSR potential with WTGs based on doubly fed induction generators (DFIG) and ac-dc-ac converter-based synchronous generators.

Appendix A
Self-Excited Double-Cage Induction Generator (SEIG) [18] Data

Power rating $= 1000$ hp; $V_{\rm LL} = 26.0$ kV; $R_s = 0.015$ p.u.; $X_{\rm Ls} = 0.091$ p.u; $R_{r1} = 0.0507$ p.u.; $R_{r2} = 0.0095$ p.u.; $X_{L1} = 0.0$ p.u.; $X_{L2} = 0.0539$ p.u.; and $X_{m12} = 0.1418$; $H_G = 0.5$. Higher generator power output is obtained by choosing an appropriate number of machines acting coherently.

Appendix B
Torsional System Data

Power $= 100$ MW; $H_T = 12.5$ p.u.; $H_G = 0.5$ p.u.; $K_{\rm GT} = 0.15$ p.u.

Appendix C
SVC Data

100-MW power transfer

$$Q_C = 150\ \text{MVAr};\ Q_L = 100\ \text{MVAr}.$$

500-MW power transfer

$$Q_C = 300\ \text{MVAr}; Q_L = 200\ \text{MVAr}.$$

Voltage regulator $K_P = 0.0; K_I = 200;$.

SSR damping controller $K_{\rm aux} = 100; K_w = 1.0; T_w = 10.0$ s.

SVC slope $= 3\%$.

Appendix D
TCSC Data

$p =$ percentage series compensation $X_C/X_\Sigma = 90\%, 65\%, 50\%; X_L$ is calculated from (5) to avoid multiple resonances in TCSC reactance-firing angle characteristics.

TCSC current controller $K_P = 0.0; K_I = 200$.

Acknowledgment

The authors gratefully acknowledge Dr. P. Pourbeik for his valuable discussions related to this work.

References

[1] P. B. Eriksen, T. Ackermann, H. Abildgaard, P. Smith, W. Winter, and J. M. Rodriguez Garcia, "System operation with high wind penetration," *IEEE Power Energy Mag.*, vol. 3, no. 6, pp. 65–74, Nov./Dec. 2005.

[2] T. Ackerman, *Power Wind Power in Power Systems*. New York: Wiley, 2005.

[3] IEEE Committee Rep., "Reader's guide to subsynchronous resonance," *IEEE Trans. Power Syst.*, vol. 7, no. 1, pp. 150–157, Feb. 1992.

[4] IEEE Working Committee Rep., "Third supplement to a bibliography for the study of subsynchronous resonance between rotating machines and power systems," *IEEE Trans. Power Syst.*, vol. 6, no. 2, pp. 830–834, May 1991.

[5] N. G. Hingorani and L. Gyugyi, *Understanding FACTS*. New York: IEEE Press, 1996.

[6] R. M. Mathur and R. K. Varma, *Thyristor-Based FACTS Controllers for Electrical Transmission Systems*. Piscataway, NJ: IEEE Press, Feb. 2002.

[7] A. E. Hammad and M. El-Sadek, "Application of a thyristor controlled VAR compensator for damping subsynchronous oscillations in power systems," *IEEE Trans. Power App. Syst.*, vol. PAS-1-3, no. 1, pp. 198–212, Jan. 1984.

[8] N. C. Abi Samra, R. F. Smith, T. E. McDermott, and M. B. Chidester, "Analysis of thyristor controlled shunt SSR counter measures," *IEEE Trans. Power App. Syst.*, vol. PAS-104, no. 3, pp. 584–597, Mar. 1985.

[9] W. Zhu, R. Spee, R. R. Mohler, G. C. Alexander, W. A. Mittelstadt, and D. Maratukulam, "An EMTP study of SSR mitigation using the thyristor controlled series capacitor," *IEEE Trans. Power Del.*, vol. 10, no. 3, pp. 1479–1485, Jul. 1995.

[10] D. G. Ramey, D. S. Kimmel, J. W. Dorney, and F. H. Kroening, "Dynamic stabilizer verification tests at the san juan station," *IEEE Trans. Power App. Syst.*, vol. PAS-100, no. 12, pp. 5011–5019, Dec. 1981.

[11] J. F. Hauer, W. A. Mittelstadt, R. J. Piwko, B. L. Damsky, and J. D. Eden, "Modulation and SSR tests performed on the BPA 500 kV thyristor controlled series capacitor unit at slatt substation," *IEEE Trans. Power Syst.*, vol. 11, no. 2, pp. 801–806, May 1996.

[12] T. Thiringer and J. A. Dahlberg, "Periodic pulsations from a three-bladed wind turbine," *IEEE Trans. Energy Convers.*, vol. 16, no. 2, pp. 128–133, Jun. 2001.

[13] E. N. Hinrichsen and P. J. Nolan, "Dynamics and stability of wind turbine generators," *IEEE Trans. Power App. Syst.*, vol. PAS-101, no. 8, pp. 2640–2648, Aug. 1982.

[14] P. Pourbeik, R. J. Koessler, D. L. Dickmander, and W. Wong, "Integration of large wind farms into utility grids (Part 2—Performance issues)," in *Proc. IEEE Power Eng. Soc. General Meeting Conf.*, 2003, pp. 1520–1525.

[15] R. K. Varma and S. Auddy, "Mitigation of subsynchronous oscillations in a series compensated wind farm using static var compensator," in *Proc. IEEE Power Eng. Soc. General Meeting Conf.*, 2006, pp. 1–7, Paper 06 GM1272.

[16] IEEE Committee Rep., "First benchmark model for computer simulation of subsynchronous resonance," *IEEE Trans. Power App. Syst.*, vol. PAS-96, no. 5, pp. 1565–1572, Sep./Oct. 1977.

[17] *"DSA Power Tools User Manual,"* Power Tech Lab, Surrey, BC, Canada, 2005.

[18] *"EMTDC PSCAD User Manual,"* HVDC Research Center, Winnipeg, MB, Canada, 2003.

[19] P. Kundur, *Power Systems Stability and Control*. New York: McGraw-Hill, 1994.

[20] J. J. Sanchez-Gasca, N. W. Miller, and W. W. Price, "A modal analysis of a two-area system with significant wind power penetration," in *Proc. IEEE Power Systems Conf. Expo.*, 2004, pp. 1–5.

[21] J. G. Slootweg and W. L. King, "Is the Answer Blowing in the Wind?," *IEEE Power Energy Mag.*, vol. 1, no. 6, pp. 26–33, Nov./Dec. 2003.

Rajiv K. Varma (M'96) received the B.Tech. and Ph.D. degrees in electrical engineering from the Indian Institute of Technology (IIT), Kanpur, India, in 1980 and 1988, respectively.

Currently, he is an Associate Professor and Associate Chair-Graduate at the University of Western Ontario (UWO), London, ON, Canada. Previously, he was a Faculty Member in the Electrical Engineering Department at the Indian Institute of Technology Kanpur, Kanpur, India, from 1989 to 2001.

Dr. Varma was awarded the Government of India BOYSCAST Young Scientist Fellowship in 1992–1993 to conduct research on flexible ac transmission systems (FACTS) at the University of Western Ontario (UWO). He also received the Fulbright Grant of the U.S. Educational Foundation in India, to conduct research in FACTS at the Bonneville Power Administration (BPA), Portland, OR, in 1998. He is the Chair of IEEE Working Group on "FACTS and HVDC Bibliography" and is active on a number of other IEEE working groups. He has received several teaching excellence awards at the Faculty of Engineering and University level at UWO. His research interests include FACTS, power systems stability, grid integration of wind and solar power systems, and distribution automation.

Soubhik Auddy (S'06) received the B.E. degree in electrical engineering from Jadavpur University, Calcutta, India, in 2000 and the M.Tech. degree in electrical engineering from the Indian Institute of Technology Kanpur, Kanpur, India, in 2003, and is currently pursuing the Ph.D. degree at the University of Western Ontario, London, ON, Canada.

His research interests include FACTS, power system dynamics, and stability.

Ysni Semsedini received the B.Sc. and M.Sc. degrees in electrical and computer engineering from the University of Western Ontario, London, ON, Canada, in 2003 and 2006, respectively.

He was a Distribution Engineer with Kitchener—Wilmot Hydro, Kitchener, ON, Canada, from 2003 to 2004. Currently, he is with London Hydro, London, ON. His research interests include modeling and performance studies of wind farms and FACTS.